An Ab Initio and Density Functional Theory Investigation of the Structures and Energetics of Halide Ion−Alcohol Complexes in the Gas Phase

B. Bogdanov and T. B. McMahon*

Department of Chemistry, University of Waterloo, Waterloo, Ontario, Canada N2L 3G1

Received: February 29, 2000; In Final Form: May 30, 2000

The gas-phase clustering equilibria of halide ions to a homologous series of alcohol molecules, $X^- + HOR \rightleftharpoons X^-(HOR)$ (X = F, Cl, Br, I; R = CH_3, CH_3CH_2, $(CH_3)_2CH$, $(CH_3)_3C$), have been investigated using ab initio (MP2(full)) and density functional theory (B3LYP) computational methods. For both methods, extended basis sets, including diffuse and polarization functions for all atoms and anions, except I^-, were used. For I^- three different effective core potentials (ECP) were used to test their suitability for these systems. Comparing the ΔH°_{298} and ΔS°_{298} values obtained with various experimental data indicates that the MP2 and MP2//B3LYP methods perform best. Structural and spectroscopic features, as well as charge distributions, show interesting trends for the various $X^-(HOR)$ complexes, and the intrinsic contributions of the halide ions and the alcohol molecules to these trends are discussed. Finally, two-dimensional potential energy surface scans were performed for the $X^-(HOCH_3)$ complexes at the MP2/6-311++G(d,p) level of theory. These surfaces reveal the asymmetric nature of the potential energy surface for the heavier halide ions, and the "floppy" nature of all the halide ion adducts.

Introduction

In the condensed phase, solvent effects are among the most important factors that determine structure−activity relationships. Examples include the lifetimes of biradicals,[1] the (non-) occurrence of exciplexes,[2] the energies of excited states,[3] the reactivity of nucleophiles and leaving groups,[4,5] ion-pair separation,[6] acidities and basicities,[7] photosentization,[8] and finally the effects on S_N1, S_N2, E1, and E2 types of reactions.[9−12] In electrochemistry the degree of ion solvation determines the ion activity and mobility, and consequently the conductivity of the electrolyte solutions. In biochemistry one of the most important solvation phenomena is the solvation of zwitterionic amino acids which renders these species significantly more stabilized than their uncharged isomers.[13] Insight into solution phenomena has been gained from thermodynamic measurements for the transfer of ions from the gas phase into the condensed phase, or from one solution to another. The most common quantity experimentally investigated is the free energy change of transfer, ΔG_{tr}, and a large amount of data concerning many different ions and solvents has been obtained.[14] These free energies of transfer frequently reveal the importance of hydrogen bonding in ion solvation. Water is the most common solvent and many of its unique chemical and physical properties are determined by the hydrogen-bonded network. Halide ions, especially chloride ion, are among the most common anions present in nature, and consequently halide ion−water interactions are among the most extensively studied systems.[15,16] Gas-phase ion chemistry has, for many decades, played an important role in studying ionic clusters and powerful techniques to generate and study micro-solvated ionic species have been developed.[17] Much insight into bulk behavior has been obtained by deducing solvent effects at a microscopic level. This has been done by investigating the thermochemistry, reactivity, and structures of solvated ions, and comparing these data with results from bare or nonsolvated ions.[15,18] One of the most extensively studied phenomena with halide ion−water clusters is the occurrence and possible competition between interior and surface solvation. Most information to date has been obtained from ab initio [16i,n,19] and molecular dynamics computations,[20] but recently, ion spectroscopy has also been used to prove existence of features that had been either speculative or based upon computations.[16a−g,k,m,21] For the last three decades an impressive amount of data on ion solvation in the gas phase has been obtained that has proven to be useful use in many diverse field of science.[22] Most of these data deals with relatively small systems, but the fundamental knowledge obtained from these small systems can, by analogy, easily be used for larger, more practical systems. One example is the field of supramolecular chemistry, where the development of anion specific host−guest systems is gaining more interest and importance.[23] Understanding these systems in the condensed phase would be difficult without the full understanding of smaller systems in the gas phase and in micro-solvated environments. There are still many features that have not received sufficient attention. Recently there has been a renewed interest in halide ion-alcohol complexes, both experimentally and theoretically.[21b,c,24] The polar, mono-protic alcohol molecules do not form extensive, hydrogen-bonded networks such as water molecules. One of the main questions for these systems is, whether interior solvation will take place in the larger halide ion-alcohol clusters. Carbacos et al. recently showed, by vibrational predissociation spectroscopy (VPDS) on $Cl^-(HOCH_3)_n$ clusters, that for $n = 4$ one of the methanol molecules is bonded to one of the three other methanol molecules that make up the so-called first solvation shell around chloride ion.[21b] It then would seem to be a logical step for future VPDS experiments to find out whether this asymmetric solvation is dependent on both the shape of the alcohol molecule and the type of halide ion.

* Corresponding author. Phone: (519) 888-4591. Fax: (519) 746-0435. E-mail: mcmahon@Uwaterloo.ca.

10.1021/jp000776m CCC: $19.00
Published on Web 07/28/2000

In the present work a systematic computational study has been performed on mono-solvated halide ion-alcohol complexes. For most of these species little or no computational data were previously available. In some cases the available computational data were obtained at higher levels of theory than the work presented here. One of the objectives was to find a level of theory that is relatively fast, and that can reproduce experimental data for halide ion-alcohol complexes well. Mono-solvated halide-ion alcohol complexes of course cannot be considered good model systems for halide-ion solvation, but if it will be possible to model mono-solvation accurately by obtaining, for instance, reliable thermochemical data, extension to larger halide-ion alcohol complexes can be made with more confidence. Those results may provide an accurate input for modeling the kinetics of the thermal unimolecular dissociation of halide ion-alcohol complexes, and to help in interpreting VPDS experiments of halide ion-alcohol complexes.

In addition, more insight into the details and trends of the structures, the IR spectroscopic characteristics, and the electronic nature of the hydrogen-bond formed would be desirable. For these kinds of systems it seemed most logical, a priori, to use theoretical methods that include electron correlation, and consequently the Møller−Plesset second-order perturbation theory including all electrons (MP2(full)),[25] and the Becke three-parameter Lee, Yang, and Parr nonlocal, exchange correlation functional (B3LYP)[26] seemed good choices in this respect. As well, these methods had been successfully applied to similar systems in the past.[21b,c,24a−c,27] The MP2 method is a very time and memory intensive method[28] compared to B3LYP, and its use is limited to systems containing a relatively small number of heavy atoms. The B3LYP method, on the other hand, can handle relatively large systems well, while using a relatively small amount of CPU time. Extended basis sets including polarization and diffuse functions were used since these have been shown to model the relatively weak noncovalent interactions within the halide ion-alcohol complexes relatively well.

Finally, two-dimensional potential energy surface scans were performed on the halide ion- methanol complexes to try to obtain some insight into the possible dynamics of halide ion-methanol complex formation, and the dynamics within the halide ion-methanol complexes.

Computational Methods

All computations were performed using the *Gaussian 94*[29] and *Gaussian 98*[30] suites of programs on a Digital Equipment Corporation (Compaq) computer (model Enterprise 2100 Alpha Server) with 4 CPU's (EV5 at 250 MHz), physical memory of 1GB, local storage of 28 GB, and Digital Unix 4.0 as operating system.

The following different computational procedures were used. For all systems studied B3LYP[26] geometry optimizations and frequency computations were performed using the 6-311+G-(d,p) (**a**) basis set,[31] as described previously.[24a] Single point energy computations on these B3LYP optimized structures were performed using MP2[25] in combination with the 6-311++G-(d,p) (**b**) basis set,[32] or using B3LYP in combination with the 6-311++G(3df,3pd) (**c**) basis set.[33] For the four halide ion-methanol complexes and fluoride ion-ethanol complex, additional computations were performed at the MP2/**a** level of theory. At this level, harmonic normal mode vibrational frequencies were scaled by 0.9489[34] to obtain thermochemical data. For the B3LYP computations, scaling factors of 1.0000[24a]

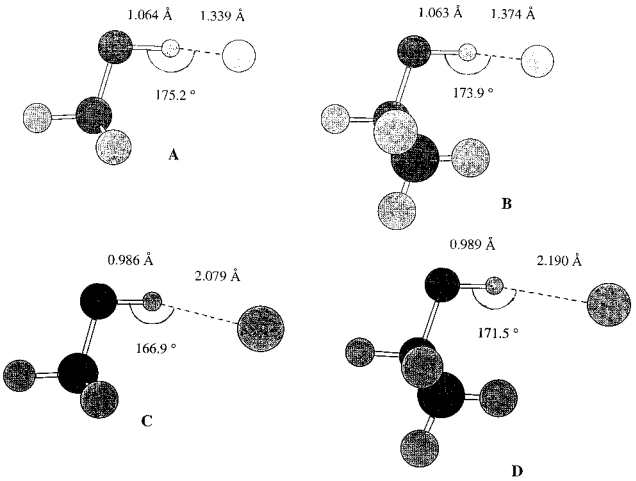

Figure 1. Optimized structures of $F^-(HOCH_3)$ (A), $Cl^-(HOCH_3)$ (C) (MP2/**a**), $F^-(HOCH(CH_3)_2)$ (B), and $Cl^-(HOCH(CH_3)_2)$ (D) (B3LYP/**b**).

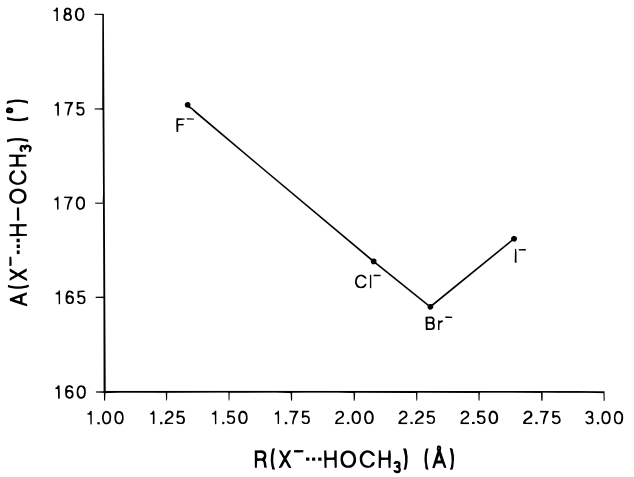

Figure 2. Plot of the MP2/**a** ([**a**/**e**] for X = I) calculated $X^-\cdots HOCH_3$ distance, $R(X^-\cdots HOCH_3)$, versus the $X^-\cdots H-OCH_3$ angle, $A(X^-\cdots H-OCH_3)$ (X = F, Cl, Br, I).

and 0.9640[35] (X = F, Cl, Br; R = CH_3, CH_2CH_3) were used. For I^-, the LanL2DZ (**d**),[36] Stuttgart RLC ECP (**e**),[37] and CRENBL ECP (**f**)[38] were used[39] in combination with the various basis sets for hydrogen, carbon, and oxygen. Natural population analysis (NPA) charges[40] were calculated for the $F^-(HOR)$ complexes (R = CH_3, CH_2CH_3, $CH(CH_3)_2$, $C(CH_3)_3$) at the B3LYP/**b** and MP2/**a**//B3LYP/**b** levels of theory, and for $X^-(HOCH_3)$ complexes (X = F, Cl, Br, I) at the MP2/**a** ([**a**/**e**] for X = I) level of theory.

Potential energy surface scans[41] for the $X^-(HOCH_3)$ complexes were performed as follows.

The structures of the $X^-(HOCH_3)$ complexes were optimized at the MP2/**a** ([**a**/**e**] for X = I) level of theory. Following this, a z-matrix was constructed with two variables: (1) the $X^-\cdots HOCH_3$ distance (R), and (2) the $X^-\cdots H-OCH_3$ angle (A) as indicated in Figure 5. A total of 352 (X = F) or 432 (X = Cl, Br, I) single point energy calculations were performed at the same levels of theory used to optimize the structures of the $X^-(HOCH_3)$ complexes by varying R and A between certain values (see Figure 6). No new geometry optimizations were performed for each step during the scan.

The calculated standard ambient enthalpy and entropy changes (ΔH°_{298} and ΔS°_{298}, respectively) of the halide ion-alcohol

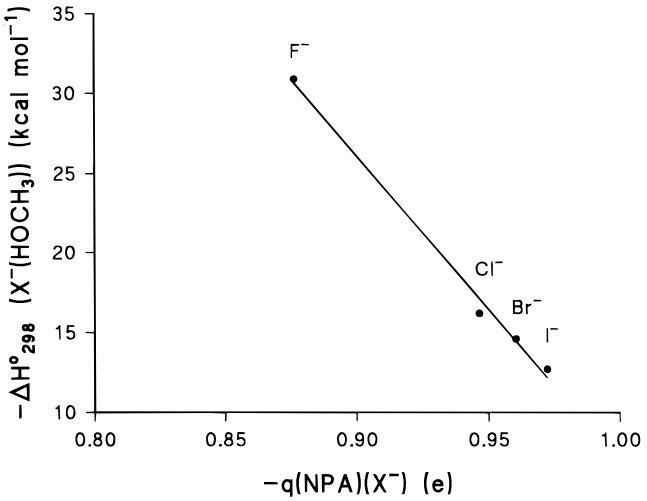

Figure 3. Plot of the MP2/**a** ([**a**/**e**] for X = I) calculated negative NPA charge on the halide, $-q(\mathrm{NPA})(X^-)$, versus the negative standard ambient enthalpy of association to form $X^-(HOCH_3)$, $-\Delta H^\circ_{298}$ ($X^-(HOCH_3)$) (X = F, Cl, Br, I).

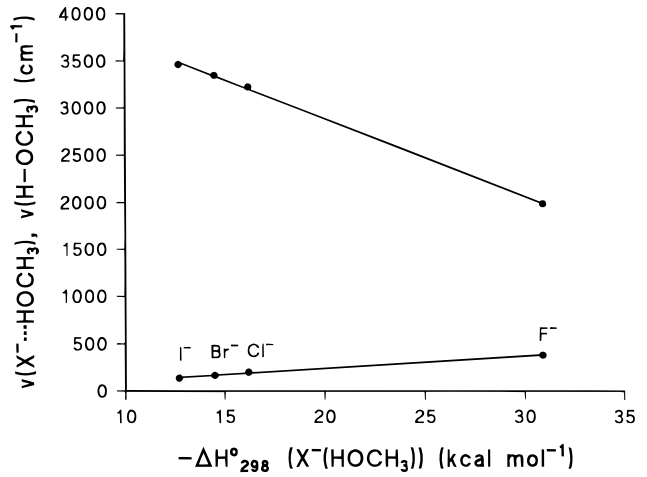

Figure 4. Plot of the MP2/**a** ([**a**/**e**] for X = I) calculated negative standard ambient enthalpy of association to form $X^-(HOCH_3)$, $-\Delta H^\circ_{298}$ ($X^-(HOCH_3)$), versus the $X^-\cdots HOCH_3$ and $H-OCH_3$ normal mode vibrational frequencies, $\nu(X^-\cdots HOCH_3)$ and $\nu(H-OCH_3)$, respectively (X = F, Cl, Br, I).

clustering equilibria (eq 1) were determined by using the following equations (eqs 2−4),

$$X^- + HOR \rightleftharpoons X^-(HOR) \quad (1)$$

$$H^\circ_{298} = E^\circ_{e,0} + \mathrm{ZPE} + \int_0^{298} C_p(T)\,dT + RT \quad (2)$$

$$S^\circ_{298} = S^\circ_0 + \int_0^{298} \frac{C_p(T)\,dT}{T} \quad (3)$$

$$C_p(T) = \frac{R}{T^2}\left(\frac{\partial^2 \ln Q}{\partial(1/T)^2}\right) + R \quad (4)$$

where $C_p(T)$ is the heat capacity at constant pressure, and Q is the total molecular partition function. ΔH°_{298} and ΔS°_{298} for eq 1 are then calculated using eq 5 and 6.

$$\Delta H^\circ_{298} = H^\circ_{298}(X^-(HOR)) - H^\circ_{298}(X^-) - H^\circ_{298}(ROH) \quad (5)$$

$$\Delta S^\circ_{298} = S^\circ_{298}(X^-(HOR)) - S^\circ_{298}(X^-) - S^\circ_{298}(ROH) \quad (6)$$

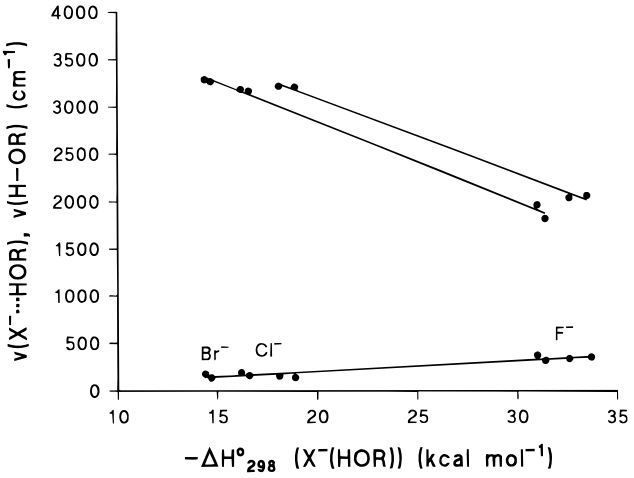

Figure 5. Plot of the MP2/**a**//B3LYP/**b** calculated negative standard ambient enthalpy of association to form $X^-(HOR)$, $-\Delta H^\circ_{298}$ ($X^-(HOR)$), versus the B3LYP/**b** $X^-\cdots HOR$ and $H-OR$ normal mode vibrational frequencies, $\nu(X^-\cdots HOR)$ and $\nu(H-OR)$, respectively (X = F, Cl, Br; R = CH_3, CH_3CH_2, $(CH_3)_2CH$, $(CH_3)_3C$).

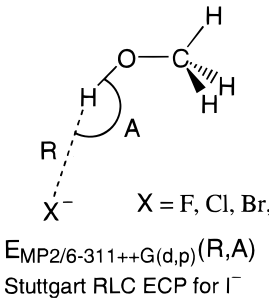

Figure 6. Definition of the $X^-\cdots HOCH_3$ distance, $R(X^-\cdots HOCH_3)$, and the $X^-\cdots H-OCH_3$ angle, $A(X^-\cdots H-OCH_3)$, parameters used for the two-dimensional potential energy surface scans at the MP2/**a** ([**a**/**e**] for X = I) level of theory (X = F, Cl, Br, I).

Results and Discussion

Structures. The structures of the $X^-(HOR)$ complexes provide interesting features that give more insight into the observed thermochemistry of $X^-(HOR)$ complex formation. Structures of the $X^-(HOCH_3)$ complexes have been published in the past,[27a−c,42b] which show minimal basis set effects. In Figure 1, the MP2/**a** structures of $F^-(HOCH_3)$ and $Cl^-(HOCH_3)$, and the B3LYP/**b** structures of $F^-(HOCH(CH_3)_2)$ and $Cl^-(HOCH(CH_3)_2)$ are shown. These were chosen, since in going from X = F to Cl, and from R = CH_3 to $(CH_3)_2CH$ the largest structural changes take place in the $X^-\cdots HOR$ bond distance and the $X^-\cdots H-OR$ bond angles. The MP2/**a** ([**a**/**d**] for X = I) structures of $X^-(HOCH_3)$ show an interesting feature. Going from X = F to Br the $X^-\cdots HOCH_3$ bond distances increase, while at the same time the $X^-\cdots H-OCH_3$ bond angles decrease as shown in Figure 2. Both these changes are mainly due to the increase in size of X^-, which will allow more interaction with the permanent dipole moment of CH_3OH as a result of the decrease in importance of a nearly linear hydrogen bonding interaction with the OH group. Going from X = Br to I one would expect an increase in the $X^-\cdots HOCH_3$ bond distance and this indeed occurs, but instead of a further decrease of the $X^-\cdots H-OCH_3$ bond angle an increase is observed, causing a break in the plot. The most likely explanation may be that I^- is so large that repulsion with the methyl group hydrogen atoms is becoming so strong that I^- is being pushed back. Changes with respect to H−OR bond length going from

ROH to X^-(HOR) (ΔR(H−OR)) for X = F, Cl, Br, I and R = CH_3, CH_3CH_2, $(CH_3)_2CH$, and $(CH_3)_3C$ can be observed that are directly related to ΔH°_{298} and frequency shifts in H−OR normal mode vibrational frequencies ($\Delta\nu$(H−OR)). For the $I^-(HOCH_3)$ complexes small differences can be found and these may be attributed to I^- basis set effects. Comparing the MP2 and B3LYP structural results for CH_3OH and the four $X^-(HOCH_3)$ complexes, only small differences are noticeable. They occur mainly in the $X^-\cdots HOCH_3$ bond distance, with B3LYP results in general being a fraction larger (+0.013 Å, +0.051 Å, +0.028 Å, and +0.019/0.026 Å for X = F, Cl, Br, and I ([**a**/**d**]/[**a**/**e**]), respectively). These differences are small enough to justify the use of B3LYP/**b** structures for MP2/**a**//B3LYP/**b** single point energy computations. As for the MP2 computations on $I^-(HOCH_3)$, the B3LYP structures also show some variation depending on the basis set for I^-. These small structural differences cannot explain the large differences in ΔH°_{298}. The B3LYP/**b** structures for X^-(HOR) (X = F, Cl; R = CH_3CH_2, $(CH_3)_2CH$, $(CH_3)_3C$) show that for both going from R = CH_3CH_2 to $(CH_3)_2CH$ a slight increase in the $X^-\cdots HOCH_3$ bond distance occurs. The main difference between the F^-(HOR) and Cl^-(HOR) complexes is that for X = F the $X^-\cdots$HOR bond angle decreases from R = CH_3CH_2 to $(CH_3)_2CH$, while for X = Cl it increases slightly.

Thermochemistry. In Tables 1 to 3 overviews are given of the computational results for association thermochemistry, together with all available experimental literature data.[17c,24a,c,27c,42] The ΔH°_{298} data from the MP2/**a** and MP2/**a**//B3LYP/**b** computations for the formation of $X^-(HOCH_3)$ (X = F, Cl, Br) and $F^-(HOCH_2CH_3)$ are identical. In general it took less CPU time to do the MP2/**a**//B3LYP/**b** computation than to do the MP2/**a** computation. Comparing the ΔH°_{298} data MP2/**a** ([**a**/**d**] and [**a**/**e**] for X = I) with the B3LYP/**b** results ([**a**/**d**], [**a**/**e**], and [**a**/**f**] for X = I) for computations for the formation of $X^-(HOCH_3)$ (X = F, Cl, Br), in general the MP2/**a** values are more negative than the B3LYP/**b** values (except for X = F). The MP2/**a** and B3LYP/**b** ΔS°_{298} values for the formation of $F^-(HOCH_3)$ and $Br^-(HOCH_3)$ are in excellent agreement, while for $F^-(HOCH_2CH_3)$ and $Cl^-(HOCH_3)$ there is a small difference. The MP2/[**a**/**d**] and [**a**/**e**] ΔH°_{298} results for $I^-(HOCH_3)$ show a large I^- basis set effect, while for the ΔS°_{298} results there is no real difference. This large I^- basis set effect on the ΔH°_{298} results for the B3LYP computations remains, with [**a**/**e**] performing the best compared to experimental results. For ΔS°_{298}, the results of [**a**/**d**] and [**a**/**e**] are nearly identical, while for [**a**/**f**] it is quite different, as was the case for the ΔH°_{298} values. Use of a modified LanL2DZ basis set,[43] the Stuttgart Dresden ECP basis set (SSD),[44] or Truhlar's SV2P+ basis set might improve results.[45] Comparing ΔH°_{298} results for B3LYP/**b** and B3LYP/**c**//B3LYP/**b** computations show that there are no real improvements. Only for $F^-(HOCH(CH_3)_2)$ and $F^-(HOC(CH_3)_3)$ the ΔH°_{298} values get −2.7 and −1.1 kcal mol^{-1} more exothermic, respectively.

Computations vs Experiments. It is of interest to compare the present computational results with pulsed-ionization high pressure mass spectrometry (PHPMS) data from this laboratory. The motivation to do so is based on the fact that previously published PHPMS data from this laboratory comprise the most extensive study on halide ion-alcohol clusters to date.[24a]

From Tables 1−3 it can easily be observed that, in general, there is good to excellent agreement between our PHPMS data and the results from MP2/**a** and MP2/**a**//B3LYP/**b** computations, but that in some cases B3LYP/**b** also performs very well. Some inconsistencies exist between the agreement of ΔH° and ΔH°_{298}, and ΔS° and ΔS°_{298}, especially for $I^-(HOCH_3)$ where I^- basis set effects are clearly observable.

Comparing these computations with other experimental results from various methods also aids in the understanding of the general performance of the different methods used for this study. If ±1.0 kcal mol^{-1} is taken as indicating good agreement between computational and experimental values, it can be concluded that the MP2/**a**//B3LYP/**b** method performs best overall. There is a good agreement with most PHPMS (88%), EPDS (50%), TCID (50%), ICR (38%), and FT-ICR (100%) data. B3LYP/**b** performs much more poorly with good agreement only in 75% of the TCID and ICR data, while B3LYP/**c**//B3LYP/**b** in general agrees poorly with all experimental data. To compare the calculated ΔS°_{298} values with ΔS° values from other experiments, it can be seen from Tables 1 to 3 that only HPMS and PHPMS experiments provide ΔS° data. Most HPMS data are in poor agreement with all calculations, and consequently they will not be considered here. The ΔS° data from ICR experiments are actually values calculated from simple statistical mechanics, and these were only used as estimates. In general there is good agreement between the MP2/**a** and B3LYP/**b** ΔS°_{298} values and the corresponding ICR values for most X^-(HOR) (X = F, Cl) clustering reactions. The spread in ΔS° values from PHPMS for Cl^-(HOR) is fairly small, and consequently the same argument applies as in comparing ΔS°_{298} and our ΔS° data. For Br^-(HOR) and $I^-(HOCH_3)$ there are too few PHPMS ΔS° values available to have a useful comparison. A general conclusion for these systems could be that it depends on the method used and the data set in order to get a good or reasonable agreement.

All B3LYP/**b** ΔH°_{298} and ΔS°_{298} values were calculated using a scaling factor of 1.0000 as described above. For some X^-(HOR) systems (X = F, Cl, Br; R = CH_3, CH_2CH_3) ΔH°_{298} and ΔS°_{298} were also calculated using a scaling factor of 0.9640. For ΔH°_{298} in general this resulted in a change of ±0.1 kcal mol^{-1}, while for ΔS°_{298} there was a change of $<+0.2$ cal mol^{-1} K^{-1}.

Other Computational Work. Various studies have been reported in the literature which deal with halide ion-alcohol molecule complexes. However, the focus here will be confined to high level ab initio results. $F^-(HOCH_3)$ has been the subject of several computational studies. The closest result to our PHPMS data is from MP2(full)/[13s8p6d4f,8s6p4d](+) + CCSD(T)/QZ(+)(2d,2p) computations by Wladkowski et al. (ΔH°_{298} = −30.0 kcal mol^{-1}).[27b] Other computations on $F^-(HOCH_3)$ include G2,[24a] and MP4(SDTQ)(fc)/6-31++G(d,p)//MP2(full)/6-311++G(d,p),[27a] but, surprisingly, these very high level computations do not give results that are more accurate, than for instance, our MP2/**a**//B3LYP/**a** results. It is possible that G2(MP2)(+) (plus ECP for Br^- and I^- containing complexes) would be more accurate than G2.[46] Recently DeTuri et al. published results on F^-(HOR) complexes.[24c] At the MP2(fc)/6-311+G(2d,p)//MP2(fc)/6-31G(d) + (ZPE + ΔC_P(298 K) at the HF/6-31G(d) level of theory, and using a scaling factor of 0.8953) they found ΔH°_{298} values of −31.8, −25.5, −33.7, and −33.2 kcal mol^{-1} for CH_3OH to $(CH_3)_3COH$, respectively.[47] With the exception of the unusual $F^-(HOCH_2CH_3)$ result, the general trend is quite reasonable. These computations could be improved by using HF/6-31++G(d,p) for ZPE + ΔC_P(298 K), and MP2(full)/6-31+G(d,p) for the geometry optimizations, but, on the other hand, this would make the computations more time-consuming.

For the Cl^-(HOR) complexes only data for $Cl^-(HOCH_3)$ and $Cl^-(HOCH(CH_3)_2)$ are available. Berthier et al. used MP2(fc)

in combination with extended Gaussian basis sets enlarged with both standard valence polarization orbitals and semidiffuse Coulomb polarization orbitals.[27d] For $Cl^-(HOCH_3)$ and $Cl^-(HOCH(CH_3)_2)$, ΔH^o_{298} values of −16.9 and −18.5 kcal mol^{-1}, respectively, were calculated. These results are in excellent agreement with our MP2/**a**//B3LYP/**b** data. After a BSSE correction, final values of −14.3 and −13.9 kcal mol^{-1}, respectively, were obtained.

This shows, that for our computations, BSSE may still be important, even though they have been neglected as indicated earlier. For $Br^-(HOCH_3)$ Tanabe et al. used a very extensive computation at the MP4(SDTQ)/[7s6p4d+ECP/D95+G(p)]//MP2(full)//[7s6p4d+ECP/D95+G(p)] level of theory and found a ΔH°_{335} value of −13.9 kcal mol^{-1}, in good agreement with their FT-ICR result.[27c] Nielsen et al. carried out computations on $I^-(HOCH_3)$ at the B3LYP/LanL2DZ+ [41] level of theory, but unfortunately no thermochemical data were reported.[21c] Thus, the various computations at high levels still give rise to results that may differ from experimental data. No HF results have been mentioned, however that does not mean that they are necessarily unreliable. HF results on halide ion-alcohol complexes have been reported that showed good agreement with experiments and higher level computations,[42b] although it was very much system dependent.

Natural Population Analysis Charges vs Thermochemistry. The halide ion-alcohol complexes studied are mainly bound through ion−dipole and ion-induced dipole interactions, $V(r)$, as given by eq 7.[48]

$$V(r) = \frac{-\mu q \cos\theta(r)}{r^2} + \frac{-\alpha q^2}{2r^4} \qquad (7)$$

Natural population analysis (NPA) charges calculated at the MP2/**a** ([**a**/**d**] for X = I) level of theory for $X^-(HOCH_3)$ (X = F, Cl, Br, I), and MP2/**a**//B3LYP/**b** and B3LYP/**b** for $F^-(HOR)$ (R = CH_3, CH_3CH_2, $(CH_3)_2CH$, $(CH_3)_3C$) show some interesting correlations between NPA charges on the halide ions and the standard enthalpy change for the $X^-(HOR)$ formation. In Figure 3 a plot of $-q$(NPA)(X^-) vs $-\Delta H^\circ_{298}$ at the MP2/**a** ([**a**/**d**] for X = I) level of theory for $X^-(HOCH_3)$ (X = F, Cl, Br, I) is shown (see Table S4). This linear correlation is expected from an examination of eq 7. It should be noted however, that for the $X^-(HOCH_3)$ complexes it is not the only linear relationship that can be obtained from the computations. For the four $X^-(HOCH_3)$ complexes the difference between the standard deprotonation enthalpies of CH_3OH, $\Delta_{acid}H^\circ_{298}$ (CH_3OH), and the standard deprotonation enthalpies of the corresponding acids of the four halide ions, $\Delta_{acid}H^\circ_{298}$ (HX), is greater than zero. This means that the proton-transfer reaction (eq 8)

$$X^- + HOCH_3 \rightarrow XH + {}^-OCH_3 \qquad (8)$$

does not take place. From the data it is clear that, even though there is no proton transfer, the binding of a halide ion to an alcohol leads to some charge transfer from the halide ion to the alcohol. This results in an elongation of the H−OCH_3 bonds within the $X^-(HOCH_3)$ complexes compared to "free" CH_3OH. This elongation can, except perhaps for the $F^-(HOR)$ complexes, not be considered as a partial proton transfer. One would expect that in order to achieve efficient proton transfer, a linear $X^-\cdots H-O$ bond would be most favorable. On this basis, except for $F^-(HOCH_3)$, the other three $X^-(HOCH_3)$ complexes show less strong hydrogen bonding. This is due to the fact that for X = Cl, Br, and I the interaction is dominated by the interaction of the charge center with the permanent dipole moment of methanol that is aligned between the C−O and O−H bonds (and not along the O−H bond). As mentioned earlier, for the $F^-(HOR)$ complexes partial proton transfer seems possible. A linear relationship has been observed between the gas-phase acidity difference of ROH and HF, $\Delta_{acid}H^\circ_{298}$ (ROH) − $\Delta_{acid}H^\circ_{298}$ (HF), and the enthalpy change for the $F^-(HOR)$ formation, ΔH°.[17c] Using ΔH°_{298} for deprotonation of ROH obtained by DeTuri et al. from TCID experiments,[24b,24c] and ΔH°_{298} for deprotonation of HF (or better $D_0(H^+-F^-)$) by Martin et al. from threshold ion-pair spectroscopy experiments,[49] and our MP2/**a**//B3LYP/**b** ΔH°_{298} values, a similar relationship can be obtained. None of these four systems qualifies as proton transfer, but one would expect that if the acidity difference between ROH and HF decreases, the amount of charge transfer would increase as discussed above. For the $F^-(HOR)$ complexes, NPA charges were calculated at the MP2/**a**//B3LYP/**b** and B3LYP/**b** levels of theory (Table S5). In general, both methods show the same trends. For the MP2/**a**//B3LYP/**b**, the NPA charge on F^- is approximately 0.029*e* more negative compared to B3LYP/**b**, while for H and O they are 0.041*e* more positive and 0.059*e* more negative, respectively. By looking at the ΔH°_{298} and q(NPA)(F^-) results (both at the MP2/**a**//B3LYP/**b** level of theory), it becomes immediately clear that the above relationship only holds for $F^-(HOCH_3)$ and $F^-(HOCH_2CH_3)$. For $F^-(HOCH(CH_3)_2)$ and $F^-(HOC(CH_3)_3)$ the expected linear relationship breaks down. This is due to the weaker, more nonlinear, hydrogen bond interactions, as evidenced by a slight increase in the $F^-\cdots HOR$ distance. This is being compensated for by a stronger ion−dipole interaction and stronger polarization interactions, due to the slight decrease in the $F^-\cdots H-OR$ angle, and a large decrease in the $F^-\cdots HC$ distance, respectively. In comparison, $F^-(HOCH_2CH_2CH_3)$ and $F^-(HOCH_2CH_2CH_2CH_3)$ would have been much better to test the relationships between $\Delta_{acid}H^\circ_{298}$ (ROH) − $\Delta_{acid}H^\circ_{298}$ (HF), ΔH°_{298}, and $-q$(NPA)(F^-), because they would show similar bonding characteristics to $F^-(HOCH_3)$ and $F^-(HOCH_2CH_3)$.[50] Finally, some predictions based on these NPA charges may be made with respect to isomeric dimer complexes. The NPA charges on F^- and O are almost identical, and so, based on simple ion−dipole interactions, it would be possible to have two different isomers for the $F^-(HOR)_2$ complexes, e.g., (ROH)F^-(HOR) and F^-(HOR)(HOR). Steric repulsion between the bulkier alkyl groups may make the first isomer more favorable for R = $(CH_3)_2CH$ and $(CH_3)_3C$. For $X^-(HOCH_3)$ (X = Cl, Br, I) the difference in $-q$(NPA)(X^-) and $-q$(NPA)(O) is such that the above suggested options seem less likely, although it cannot be excluded completely. Many factors will eventually determine which structures may (co-)exist.

Vibrational Frequencies. Scaling factors were introduced to the MP2/**a** and B3LYP/**b** harmonic normal mode vibrational frequncies of CH_3OH in order to match the experimental values.[51] These scaling factors were used for all subsequent ROH and $X^-(HOR)$ computations and in general good agreement was found between our results, results from a scaled quantum mechanical (SQM) force field method,[27b] and the HF/6-31G(d) (scaling factor 0.8953).[24c] For CH_3CH_2OH, $(CH_3)_2CHOH$, and $(CH_3)_3COH$ in general there is good agreement between the MP2/**a**, B3LYP/**b** and HF/6-31G(d) (0.8953) results. For the $F^-(HOCH_3)$ complex frequencies, various results have been published in the literature,[24c,27a,b] and most data show some spread in individual frequencies caused by basis set effects, but none of the methods used produced extreme deviations. Based on matching thermochemical data such as ΔH°_{298}, it would be hard to assess the quality of the vibrational frequencies.

TABLE 1: Overview of Computational MP2/a, MP2/a//B3LYP/b, B3LYP/b, and B3LYP/c//B3LYP/b Plus Experimental Thermochemistry for $X^- + ROH \rightleftharpoons X^-(HOR)$ Equilibria (X = F; R = CH_3, CH_3CH_2, $(CH_3)_2CH$, $(CH_3)_3C$; a = 6-311++G(d,p), b = 6-311+G(d,p), c = 6-311++G(3df,3pd))

X	ROH	method	ΔH°_{298} [a]	ΔS°_{298} [b]	method[c]	ΔH° [a]	ΔS° [b]	ref
F	CH_3OH	MP2/**a**	−30.9	−22.9	ICR	−29.6	−22.6	17c
		MP2/**a**//B3LYP/**b**	−31.0		PHPMS	−30.5 ± 0.7	−23.4 ± 1.2	42a
		B3LYP/**b**	−31.6	−22.6	PHPMS	−23.3	−25.0	42b
		B3LYP/**c**//B3LYP/**b**	−32.6		EPDS	−29.6 ± 0.5		42c
					TCID	−29.4 ± 2.1		24c
F	CH_3CH_2OH	MP2/**a**	−32.1	−24.6	ICR	−31.5	−24.9	
		MP2/**a**//B3LYP/**b**	−32.0		PHPMS	−32.4 ± 0.5	−25.7 ± 1.3	17c
		B3LYP/**b**	−32.4	−22.2	TCID	−32.5 ± 0.7		24a
		B3LYP/**c**//B3LYP/**b**	−33.6					24c
F	$(CH_3)_2CHOH$	MP2/**a**//B3LYP/**b**	−33.2		ICR	−32.2	−25.6	17c
		B3LYP/**b**	−32.5	−24.6	PHPMS	−33.5 ± 0.7	−26.2 ± 1.3	24a
		B3LYP/**c**//B3LYP/**b**	−35.2		TCID	−33.2 ± 0.7		24c
F	$(CH_3)_3COH$	MP2/**a**//B3LYP/**b**	−34.1		ICR	−33.3	−26.1	17c
		B3LYP/**b**	−33.4	−25.5	PHPMS	−33.4 ± 0.7	−24.8 ± 1.2	24a
		B3LYP/**c**//B3LYP/**b**	−34.5		TCID	−32.7 ± 0.7		24c

[a] In kcal mol^{-1}. [b] In cal mol^{-1} K^{-1}. [c] ICR: ion cyclotron resonance. EPDS: electron photodetachment spectroscopy. HPMS: high-pressure mass spectrometry. TCID: threshold collision induced dissociation. PHPMS: pulsed-ionization high-pressure mass spectrometry. FT-ICR: Fourier transform ion cyclotron resonance.

It would, of course, be better to have experimental vibrational data on $F^-(HOCH_3)$ and other $F^-(HOR)$ complexes. Unfortunately these are not available, and the nature of these systems (mainly due to the very strong bond involved) seems to prevent the use of VPDS to obtain them. For the $F^-(HOR)$ complexes (R = CH_3CH_2, $(CH_3)_2CH$, $(CH_3)_3C$), only our MP2/**a** (R = CH_3CH_2 only), B3LYP/**b**, and the HF/6-31G(d) (0.8953) data by DeTuri et al. are available.[24c] Once again the agreement is in general good, except for the lowest vibrational frequencies of $F^-(HOCH_3)$ and $F^-(HOC(CH_3)_3)$. Our computations used a hindered torsional methyl group rotation, while the HF/6-31G(d) results by DeTuri et al. were corrected for free methyl group rotations, which is more accurate at temperatures normally used for these types of PHPMS experiments. Better agreement might be obtained by adding diffuse and polarization functions to the hydrogen atoms. For the $Cl^-(HOCH_3)$ cluster, experimental VPDS data are available,[21b] and so this is an excellent opportunity to test different theoretical models. For the intermolecular $Cl^-\cdots HOCH_3$ stretch, Carbacos et al. found indirectly a value of 232 cm^{-1}, while for the $H-OCH_3$ stretch a value of 3162 cm^{-1} was obtained. Both the MP2/**a** (199 cm^{-1}) and B3LYP/**b** (190 cm^{-1}) results for the $Cl^-\cdots HOCH_3$ stretch are closer to the experimental VPDS results than the LMP2/cc-pVDZ result (307 cm^{-1}) obtained by the same authors. For the $H-OCH_3$ stretch the B3LYP/**b** result is in very good agreement (3186 cm^{-1}) as is the LMP2/cc-pVDZ result (3198 cm^{-1}), while the MP2/**a** results are somewhat off (3223 cm^{-1}). Unfortunately for the other three $Cl^-(HOR)$ complexes, and both $Br^-(HOR)$ complexes no VPDS data are available. Comparing the MP2/**a** and B3LYP/**b** harmonic vibrational frequencies with results from MP2(full)/[7s6p4d+ECP/D95+(p)] computations[27c] shows varying agreement. For $I^-(HOR)$ (R = CH_3, CH_3CH_2, $(CH_3)_2CH$), recently VPDS data have been published.[21c] Scaled B3LYP/LanL2DZ+ frequencies (based on matching the CH_3OH O−H stretch in the gas phase) gave excellent agreement for both the $I^-\cdots HOCH_3$ stretch (166 cm^{-1} vs 157 cm^{-1}) and the CH_3O-H stretch (3331 cm^{-1} vs 3365 cm^{-1}). It is difficult to determine why the MP2/[**a**/**e**] and B3LYP/[**b**/**e**] results are somewhat off, since it seems they fit the other observed trends well. A different basis set for I^-, and introducing correction for anharmonic low-frequency vibrational modes may improve this situation somewhat.

Vibrational Frequencies vs Thermochemistry. In Table 4 an overview is given of the ΔH°_{298} values for the different halide ion-alcohol thermochemistry, and the $X^-\cdots HOR$ and H−OR stretch vibrations of the different $X^-(HOR)$ complexes. In Figures 4 and 5 these data are plotted for the MP2/**a** ([**a**/**d**] for X = I) ($-\Delta H^\circ_{298}$ and frequencies) and MP2/**a**//B3LYP/**b** ($-\Delta H^\circ_{298}$ and B3LYP/**b** frequencies) results. As can be seen for the MP2/**a** results for $X^-(HOCH_3)$, excellent correlation between $-\Delta H^\circ_{298}$ and the $X^-\cdots HOCH_3$ and $H-OCH_3$ stretch vibrations has been obtained. This is in agreement with similar experimental results by Ayotte et al. for $X^-(H_2O)$ complexes (X = Cl, Br, I).[16b] By using experimental VPMS data for $Cl^-(HOCH_3)$ [21b] and $I^-(HOCH_3)$,[21c] and ΔH° values obtained by PHPMS,[24a] one would expect $X^-\cdots HOCH_3$ and $H-OCH_3$ stretch vibrations for X = F and Br to be 385 cm^{-1} and 2769 cm^{-1}, and 197 cm^{-1} and 3252 cm^{-1}, respectively. For $F^-\cdots HOCH_3$ and $H-OCH_3$ (in $Br^-(HOCH_3)$) these predictions, based on experimental data and assuming similar linear correlations as obtained by computation, would be in excellent agreement with our MP2/**a** computations (380 cm^{-1} and 3247 cm^{-1}, respectively). There is a notable deviation for $H-OCH_3$ (in $F^-(HOCH_3)$) and $Br^-\cdots HOCH_3$ which seems somewhat strange. The $X^-\cdots HOCH_3$ stretch vibrations cannot be observed experimentally, but can be deduced from VPDS experiments since they appear in a combination band with the $H-OCH_3$ stretch. This means that for $F^-(HOCH_3)$ and $Br^-(HOCH_3)$ bands at 3154 cm^{-1} and 3449 cm^{-1} would be observed, respectively. In Figure 5 it can be seen that a similar linear correlation exists for $-\Delta H^\circ_{298}$ and the $X^-\cdots HOR$ and H−OR stretch vibrations using $-\Delta H^\circ_{298}$ from the MP2/**a**//B3LYP/**b** level computations and B3LYP/**b** frequencies. For $X^-(HOR)$ (X = F, Cl; R = $(CH_3)_2CH$, $(CH_3)_3C$) the H−OR stretch vibrations do not lie on the line for the other $X^-(HOR)$ (X = F, Cl, Br, I; R = CH_3, CH_3CH_2) complexes. This is caused by the fact that for R = $(CH_3)_2CH$, $(CH_3)_3C$ the $X^-\cdots HOR$ stretch vibration is no longer a simple motion. There is also a motion "toward" the CH_3 groups giving rise to a smaller than expected shift to lower wavenumber, based on $-\Delta H^\circ_{298}$. Unfortunately no VPDS data for these systems are available to test these computations. The origin of the shift in H−OR stretch vibration in $X^-(HOR)$ compared to "free" ROH is mainly the result of the increase the H−OR bond length in $X^-(HOR)$ compared to "free" ROH. This increase in bond length is of course related to ΔH°_{298}, which is related, as shown previously, to the amount of charge transfer and the size of the halide ion. This relationship applies to all MP2/**a** ([**a**/**d**] for X = I) computations for the $X^-(HOR)$

TABLE 2: Overview of Computational MP2/a, MP2/a//B3LYP/b, B3LYP/b, and B3LYP/c//B3LYP/b Plus Experimental Thermochemistry for $X^- + ROH \rightleftharpoons X^-(HOR)$ Equilibria (X = Cl; R = CH_3, CH_3CH_2, $(CH_3)_2CH$, $(CH_3)_3C$; a = 6-311++G(d,p), b = 6-311+G(d,p), c = 6-311++G(3df,3pd))

X	ROH	method	ΔH°_{298} [a]	ΔS°_{298} [b]	method	ΔH° [a]	ΔS° [b]	ref
Cl	CH_3OH	MP2/**a**	−16.6	−20.1	HPMS	−14.1	−14.8	42d
		MP2/**a**//B3LYP/**b**	−16.6		HPMS	−14.2	−14.8	42e
		B3LYP/**b**	−14.9	−19.2	ICR	−16.8	−22.9	42f
		B3LYP/**c**//B3LYP/**b**	−14.9		PHPMS	−17.5 ± 0.1	−22.0 ± 0.2	42g
					PHPMS	−17.4	−24.1	42h
					PHPMS	−17.1 ± 0.1	−22.6 ± 0.1	41i
					EPDS	−18.7 ± 0.5		42c
					PHPMS	−17.5 ± 0.3	−24.0 ± 0.7	24a
Cl	CH_3CH_2OH	MP2/**a**//B3LYP/**b**	−17.2		ICR	−17.3	−23.1	42f
		B3LYP/**b**	−14.9	−19.5	PHPMS	−17.6	−23.7	42h
		B3LYP/**c**//B3LYP/**b**	−15.5		PHPMS	−17.9 ± 0.4	−24.3 ± 0.9	24a
Cl	$(CH_3)_2CHOH$	MP2/**a**//B3LYP/**b**	−18.7		ICR	−17.6	−23.3	42f
		B3LYP/**b**	−14.8	−23.2	PHPMS	−18.3	−24.7	42h
		B3LYP/**c**//B3LYP/**b**	−15.3		PHPMS	−19.4 ± 0.2	−27.1 ± 0.5	24a
Cl	$(CH_3)_3COH$	MP2/**a**//B3LYP/**b**	−19.5		HPMS	−14.2	−10.3	42d
		B3LYP/**b**	−15.3	−23.7	PHPMS	−19.2	−27.0	42j
		B3LYP/**c**//B3LYP/**b**	−15.7		ICR	−18.1	−23.4	42f
					PHPMS	−19.8	−27.4	42h
					PHPMS	−20.2 ± 0.4	−28.9 ± 1.0	24a

[a] In kcal mol^{-1}. [b] In cal mol^{-1} K^{-1}.

TABLE 3: Overview of Computational MP2/a, MP2/a//B3LYP/b, B3LYP/b, and B3LYP/c//B3LYP/b Plus Experimental Thermochemistry for $X^- + ROH \rightleftharpoons X^-(HOR)$ Equilibria (X = Br, I; R = CH_3, CH_3CH_2; a = 6-311++G(d,p), b = 6-311+G(d,p), c = 6-311++G(3df,3pd), d = LanL2DZ, e = Stuttgart RLC ECP, f = CRENBL ECP)

X	ROH	method	ΔH°_{298} [a]	ΔS°_{298} [b]	method	ΔH° [a]	ΔS° [b]	ref
Br	CH_3OH	MP2/**a**	−14.6	−19.5	PHPMS	−13.9	−17.6	42b
		MP2/**a**//B3LYP/**b**	−14.5		EPDS	−15.1 ± 0.4		42c
		B3LYP/**b**	−12.2	−19.5	PHPMS	−14.5 ± 0.1	−21.9 ± 0.4	24a
		B3LYP/**c**//B3LYP/**b**	−12.4					
Br	CH_3CH_2OH	MP2/**a**//B3LYP/**b**	−14.7		FT-ICR	−14.4		27c
		B3LYP/**b**	−12.5	−19.9	EPDS	−15.2 ± 0.6		42c
		B3LYP/**c**//B3LYP/**b**	−12.6		PHPMS	−14.1 ± 0.2	−19.8 ± 0.4	24a
I	CH_3OH	MP2/[**a**/**d**]	−17.7	−20.0	PHPMS	−11.3	−17.8	42k
		MP2/[**a**/**e**]	−12.7	−19.6	PHPMS	−11.2	−17.1	42b
		B3LYP/[**b**/**d**]	−14.4	−17.6	EPDS	−14.4 ± 0.4		42c
		B3LYP/[**c**/**d**]//B3LYP/[**b**/**d**]	−15.2		PHPMS	−11.9 ± 0.2	−20.6 ± 0.5	24a
		B3LYP/[**b**/**e**]	−10.1	−18.3				
		B3LYP/[**c**/**e**]//B3LYP/[**b**/**e**]	−10.0					
		B3LYP/[**b**/**f**]	−16.5	−23.3				
		B3LYP/[**c**/**f**]//B3LYP/[**b**/**f**]	−18.2					

[a] In kcal mol^{-1}. [b] In cal mol^{-1} K^{-1}.

TABLE 4: Overview of ΔH°_{298} for the $X^- + ROH \rightleftharpoons X^-(HOR)$ Equilibria, and the $\nu(X^-\cdots HOR)$ and $\nu(H-OR)$ Harmonic Vibrational Frequencies of the $X^-(HOR)$ Complexes (X = F, Cl, Br, I; R = CH_3, CH_3CH_2, $(CH_3)_2CH$, $(CH_3)_3C$; a = 6-311++G(d,p), b = 6-311+G(d,p), e = Stuttgart RLC ECP)

X	ROH	method	ΔH°_{298} [a]	$\nu(X^-\cdots HOR)$ [b]	$\nu(H-OR)$ [b]
F	CH_3OH	MP2/**a**	−30.9	380	1988
F	CH_3OH	MP2/**a**//B3LYP/**b**	−31.0	374[c]	1968[c]
F	C_2H_5OH	MP2/**a**	−32.1	337	1761
F	C_2H_5OH	MP2/**a**//B3LYP/**b**	−32.0	319[c]	1824[c]
F	$(CH_3)_2CHOH$	MP2/**a**//B3LYP/**b**	−33.2	339[c]	2044[c]
F	$(CH_3)_3COH$	MP2/**a**//B3LYP/**b**	−34.1	356[c]	2067[c]
Cl	CH_3OH	MP2/**a**	−16.6	199	3223
Cl	CH_3OH	MP2/**a**//B3LYP/**b**	−16.6	190[c]	3186[c]
Cl	C_2H_5OH	MP2/**a**//B3LYP/**b**	−17.2	160[c]	3168[c]
Cl	$(CH_3)_2CHOH$	MP2/**a**//B3LYP/**b**	−18.7	155[c]	3220[c]
Cl	$(CH_3)_3COH$	MP2/**a**//B3LYP/**b**	−19.5	139[c]	3211[c]
Br	CH_3OH	MP2/**a**	−14.5	165	3347
Br	CH_3OH	MP2/**a**//B3LYP/**b**	−14.4	176[c]	3288[c]
Br	C_2H_5OH	MP2/**a**//B3LYP/**b**	−14.7	137[c]	3268[c]
I	CH_3OH	MP2/[**a**/**e**]	−12.7	135	3463
I	CH_3OH	B3LYP/[**b**/**e**]	−10.1	139[d]	3402[d]

[a] In kcal mol^{-1}. [b] In cm^{-1}. [c] B3LYP/**b** frequencies. [d] B3LYP/[**b**/**e**] frequencies.

complexes (X = F, Cl, Br, I; R = CH_3, CH_3CH_2 (X = F only)), and all B3LYP/**b** computations for the $X^-(HOR)$ complexes (X = F, Cl; R = CH_3, CH_3CH_2, $(CH_3)_2CH$, $(CH_3)_3C$). It was surprising that when plotting $-\Delta H^\circ_{298}$ vs $\nu(H-OH)$ in $X^-(HOR)$, the data for R = $(CH_3)_2CH$ and $(CH_3)_3C$ would deviate from R = CH_3 and CH_3CH_2, but by plotting $\Delta R(H-OR)$ vs $\Delta\nu(H-OR)$ this deviation disappears for all alkyl groups. The magnitude of the $X^-\cdots HOR$ bond distance is directly related

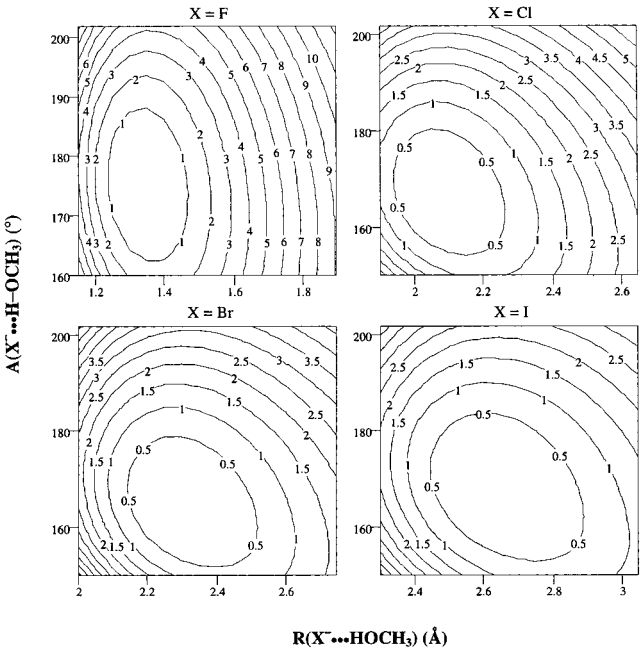

Figure 7. Plots of the MP2/**a** ([**a**/**e**] for X = I) $X^-(HOCH_3)$ two-dimensional potential energy surface (X = F, Cl, Br, I) (contour lines in kcal mol^{-1}).

to ΔH°_{298}, which is further related to the size of the halide ion. One main conclusion in this respect may be, that by simply changing the halide ion no other property in a halide ion-alcohol complexes changes. Thus different parameters are related and they cooperate in such a manner that the net result may look like one linear correlation.

Potential Energy Surfaces. In Figure 6 the two parameters which are used to obtain the four MP2/**a** ([**a**/**d**] for X = I) potential energy surfaces for $X^-(HOCH_3)$, shown in Figure 7, are defined. The contour lines represent the energies in kcal mol^{-1}, relative to the minimum energy position. It is very clear that the curve for X = F shows the least asymmetrical potential energy surface features. This is what one would expect from a hydrogen bonded system, with a linear or near linear X⁻•••H–O alignment. For X = Cl, Br, and I the potential energy surfaces are less steep, due to the smaller ΔH°_{298} values compared to X = F, and there are more asymmetric features visible. All four potential energy surfaces show clearly that the halide is quite "floppy" and loosely bound. Converting the intramolecular $X^-•••HOCH_3$ stretch vibration from cm^{-1} to kcal mol^{-1} (E = 1.08, 0.57, 0.47, and 0.39 kcal mol^{-1} for X = F, Cl, Br, and I, respectively), shows that if this motion is in its ground state, the halide ion can move freely across a fairly large distance and angle. It had been hoped that from these potential energy surfaces some clear and distinct features would be observable that would indicate how the halides ion get captured by methanol. Only for the $F^- + HOCH_3 \rightleftharpoons F^-(HOCH_3)$ complex formation is this fairly evident. The more asymmetric nature of the potential energy surfaces for the other three halide ions makes such a simplistic approach impossible.

Conclusions

Ab initio and density functional theory computations to model the thermochemistry of halide ion-alcohol clustering equilibria, $X^- + HOR \rightleftharpoons X^-(HOR)$ (X = F, Cl, Br, I; R = CH_3, CH_3CH_2, $(CH_3)_2CH$, $(CH_3)_3C$), indicate that MP2/**a** results for ΔH°_{298} and ΔS°_{298} are closer to PHPMS results for ΔH° and ΔS° than are the B3LYP/**b** results. For the larger alcohol molecules (R = $(CH_3)_2CH$, $(CH_3)_3C$) MP2/**a**//B3LYP/**b** computations perform very well to obtain accurate ΔH°_{298} values. For I^- several ECP basis sets were used and for both MP2 and B3LYP the Stuttgart RLC ECP (**e**) performed best. Natural population analysis charge computations for $X^-(HOCH_3)$ at the MP2/**a** level of theory show some charge transfer for all halide ions that is related to the ΔH°_{298} values for the clustering equilibria. For the $F^-(HOR)$ complexes this relationship breaks down going from R = CH_3CH_2 to $(CH_3)_2CH$ because stronger F⁻•••HC interactions become possible. Shifts in the H–OR normal mode vibrational frequencies are related to the elongation of the H–OR bond in the $X^-(HOR)$ complexes compared to "free" ROH. Good agreement with normal mode vibrational frequencies from other computations is obtained for most ROH molecules and $X^-(HOR)$ complexes, and with experimental VPDS results on $Cl^-(HOCH_3)$ and $I^-(HOCH_3)$. Going from X = F to Br for $X^-(HOCH_3)$, at the MP2/**a** level of theory it is shown that the X⁻•••H–OCH_3 angle decreases while the X⁻•••$HOCH_3$ distance increases due to the larger halide ion radius. For X = I the X⁻•••$HOCH_3$ distance increases, but the X⁻•••H–OCH_3 angle increased instead.

Finally, two-dimensional potential energy surfaces have been presented for the $X^-(HOCH_3)$ complexes indicating a nearly symmetric, hydrogen-bonded surface for X = F, while for X = Cl to I the potential energy surface becomes more asymmetric due to the increased importance of other interaction, most likely ion–dipole and the ion-induced dipole interactions, relative to hydrogen bonding. The surfaces confirm the "floppy" nature of the halide ion motion relative to the alcohol, but do not give any clear insight into possible trajectories and dynamics of halide ion-alcohol complex formation.

Acknowledgment. The authors would like to thank Professors M. A. Johnson and F. Tureček, Dr. K. Norrman, Dr. V. F. DeTuri, and Dr. S. B. Nielsen for help and useful suggestions with the computations, and for communication of results prior to publication. Financial support from the Natural Sciences and Engineering Research Council of Canada (NSERC) is also gratefully acknowledged.

Supporting Information Available: Scaled MP2 (Table S1) and B3LYP (Tables S2 and S3) frequencies, NPA charges of X^-(HOCH3) (Table S4) and F^-(HOR) (Table S5). This material is available free of charge via the Internet at http://pubs.acs.org. Electronic energies and entropies, and structural data of the optimized geometries are available upon request from the authors.

References and Notes

(1) Scaiano, J. C. *Acc. Chem. Res.* **1982**, *15*, 252.
(2) Eriksen, J.; Foote, C. S. *J. Am. Chem. Soc.* **1980**, *102*, 6083.
(3) Wagner, P. J.; May, M. J.; Haug, A.; Graber, D. R. *J. Am. Chem. Soc.* **1970**, *92*, 5269.
(4) Bernasconi, C. F. *Acc. Chem. Res.* **1978**, *11*, 147.
(5) Landini, D.; Maia, A.; Montanari, F.; Rolla, F. *J. Org. Chem.* **1983**, *48*, 3774.
(6) *(6)Ions and Ion Pairs in Organic Reactions*; Szwarc, M., Ed.; Wiley: New York, 1972 and 1974; Vol. 1 and Vol. 2.
(7) *(7)Mechanisms and Theory in Organic Chemistry*, 3rd ed.; Lowry, T. H., Schueller-Richardson, K., Ed.; Harper & Row: New York, 1987; Chapter 3.
(8) Ladwig, C. C.; Lui, R. S. H. *J. Am. Chem. Soc.* **1974**, *96*, 6210 and references therein.
(9) (a) Grunwald, E.; Winstein, S. *J. Am. Chem. Soc.* **1948**, *70*, 1948. (b) Schleyer, P. v. R.; Raber, D. J.; Harris, J. M. *J. Am. Chem. Soc.* **1971**, *93*, 4829 and references therein. (c) Bentley, T. W.; Carter, G. E. *J. Am. Chem. Soc.* **1982**, *104*, 5741.
(10) (a) Parker, A. J.; Mayer, U.; Schmidt, R.; Gutmann, V. *J. Org. Chem.* **1978**, *43*, 1843. (b) Shaik, S. S. *J. Am. Chem. Soc.* **1984**, *106*, 1227.

(11) (a) Cooper, K. A.; Hughes, E. D.; Ingold, C. K. *J. Chem. Soc.* **1973**, 1280. (b) Seib, R. C.; Shiner, V. J.; Sendijarević, V.; Humski, J. *J. Am. Chem. Soc.* **1978**, *100*, 8133 and references therein. (c) Richard, J. P.; Jencks, W. P. *J. Am. Chem. Soc.* **1984**, *106*, 1383. (d) Cohen, T.; Daniewski, A. R. *J. Am. Chem. Soc.* **1969**, *91*, 533. (e) Skell, P. S.; Hall, W. L. *J. Am. Chem. Soc.* **1963**, *85*, 2851.

(12) (a) Bunnett, J. F. *Angew. Chem., Int. Ed. Engl.* **1962**, *1*, 225. (b) Baciocchi, E.; Perucci, P.; Rol, C. *J. Chem. Soc. Perkin Trans. 2* **1975**, *2*, 329. (c) Beltrame, P.; Biale, G.; Lloyd, D. J.; Parker, A. J.; Ruane, M.; Winstein, S. *J. Am. Chem. Soc.* **1972**, *94*, 2240. (d) Ford, W. T.; Pietsek, D. J. J. *J. Am. Chem. Soc.* **1975**, *97*, 2194 and references therein.

(13) (a) Jensen, J. H.; Gordon, M. S. *J. Am. Chem. Soc.* **1995**, *117*, 8159. (b) Jensen, F. *J. Am. Chem. Soc.* **1992**, *114*, 9533.

(14) (a) Marcus, Y. *Pure Appl. Chem.* **1983**, *55*, 977. (b) Marcus, Y. *Pure Appl. Chem.* **1985**, *57*, 1103.

(15) Takashima, K.; Riveros, J. M. *Mass Spectrom. Rev.* **1998**, *17*, 409 and reference cited therein.

(16) (a) Bailey, C. G.; Kim, J.; Dessent, C. E. H.; Johnson, M. A. *Chem. Phys. Lett.* **1997**, *269*, 122. (b) Ayotte, P.; Bailey, C. G.; Weddle, G. H.; Johnson, M. A. *J. Phys. Chem. A* **1998**, *102*, 3067. (c) Choi, J.-H.; Kuwata, K. T.; Cao, Y.-B.; Okumura, M. *J. Phys. Chem. A* **1998**, *102*, 503. (d) Ayotte, P.; Weddle, G. H.; Kim, J.; Johnson, M. A. *Chem. Phys.* **1998**, *239*, 485. (e) Ayotte, P.; Weddle, G. H.; Kim, J.; Johnson, M. A. *J. Am. Chem. Soc.* **1998**, *120*, 12361. (f) Ayotte, P.; Weddle, G. H.; Kim, J.; Kelly, J.; Johnson, M. A. *J. Phys. Chem A* **1999**, *103*, 443. (g) Cabarcos, O. M.; Weinheimer, C. J.; Lisy, J. M.; Xantheas, S. S. *J. Chem. Phys.* **1999**, *110*, 5. (h) Weis, P.; Kemper, P. R.; Bowers, M. T.; Xantheas, S. S. *J. Am. Chem. Soc.* **1999**, *121*, 3571. (i) Dorsett, H. E.; Watts, R. O.; Xantheas, S. S. *J. Phys. Chem. A* **1999**, *103*, 3351. (j) Bryce, R. A.; Vincent, M. A.; Hillier, I. A. *J. Phys. Chem. A* **1999**, *103*, 4094. (k) Ayotte, P.; Weddle, G. H.; Johnson, M. A. *J. Chem. Phys.* **1999**, *110*, 7129. (l) Stuart, S. J.; Berne, B. J. *J. Phys. Chem. A* **1999**, *103*, 10300. (m) Ayotte, P.; Nielsen, S. B.; Weddle, G. H.; Johnson, M. A.; Xantheas, S. S. *J. Phys. Chem. A* **1999**, *103*, 10665. (n) Topol, I. A.; Tawa, G. J.; Burt, S. K.; Rashin, A. A. *J. Chem. Phys.* **1999**, *111*, 10998. (o) Majumdar, D.; Kim, J.; Kim, K. S. *J. Chem. Phys.* **2000**, *112*, 101.

(17) (a) Blair, L. K.; Isolani, P. C.; Riveros, J. M. *J. Am. Chem. Soc.* **1973**, *95*, 1057. (b) Ridge, D. P.; Beauchamp, J. L. *J. Am. Chem. Soc.* **1974**, *96*, 3595. (c) Larson, J. W.; McMahon, T. B. *J. Am. Chem. Soc.* **1983**, *105*, 2944. (d) Larson, J. W.; McMahon, T. B. *Can. J. Chem.* **1984**, *62*, 675. (e) Riveros, J. M.; Ingemann, S.; Nibbering, N. M. M. *J. Am. Chem. Soc.* **1991**, *113*, 1053. (f) Haberland, H.; Schindler, H. G.; Worsnop, D. R. *Ber. Bunsen-Ges. Phys. Chem.* **1984**, *88*, 270. (g) Coe, J. C.; Snodgrass, H. G.; Freidhoff, C. B.; McHugh, K. M.; Bowen, K. H. *J. Chem Phys.* **1987**, *87*, 4302.

(18) Viggiano, A. A.; Arnold, S. T.; Morris, R. A. *Int. Rev. Phys. Chem.* **1998**, *17*, 147 and references therein.

(19) (a) Combariza, J. E.; Kestner, N. R.; Jortner, J. *Chem Phys. Lett.* **1993**, *203*, 423. (b) Combariza, J. E.; Kestner, N. R.; Jortner, J. *J. Chem. Phys.* **1994**, *100*, 2851. (c) Xantheas, S. S.; Dunning, T. H., Jr. *J. Phys. Chem.* **1994**, *98*, 13489. (d) Xantheas, S. S.; Dang, L. X. *J. Phys. Chem.* **1996**, *100*, 3989. (e) Xantheas, S. S. *J. Phys. Chem.* **1996**, *100*, 9703.

(20) (a) Asada, T.; Nishimoto, K.; Kitaura, K. *J. Phys. Chem.* **1993**, *97*, 7724. (b) Sremaniak, L. S.; Perera, L.; Berkowitz, M. L. *Chem. Phys. Lett.* **1994**, *218*, 377. (c) Tuñón, I.; Martins-Costa, M. T. C.; Millot, C.; Ruiz-López, M. F. *Chem Phys. Lett.* **1995**, *241*, 450. (d) Bryce, R. A.; Vincent, M. A.; Hillier, I. H. *J. Phys. Chem. A* **1999**, *103*, 4094 and references therein. (e) Stuart, S. J.; Berne, B. J. *J. Phys. Chem. A* **1999**, *103*, 10300 and references therein.

(21) (a) Johnson, M. S.; Kuwata, K. T.; Wong, C.-K.; Okumura, M. *Chem. Phys. Lett.* **1996**, *260*, 551. (b) Cabarcos, O. M.; Weinheimer, C. J.; Martinez, T. J.; Lisy, J. M. *J. Chem. Phys.* **1999**, *110*, 9516. (c) Nielsen, S. B.; Ayotte, P.; Kelley, J. A.; Johnson, M. A. *J. Chem. Phys.* **1999**, *111*, 9593. (d) Ayotte, P.; Nielsen, S. B.; Weddle, G. H.; Johnson, M. A.; Xantheas, S. S. *J. Phys. Chem. A* **1999**, *103*, 10665.

(22) (a) Castleman, A. W., Jr. *Int. J. Mass Spectrom. Ion. Proc.* **1992**, *118/119*, 167. (b) Castleman, A. W., Jr.; Wei, S. *Ann. Rev. Phys. Chem.* **1994**, *45*, 685. (c) Castleman, A. W., Jr.; Bowen, K. H. *J. Phys. Chem.* **1996**, *100*, 12911.

(23) (a) Jung, M. E.; Xia, H. *Tetrahedron Lett.* **1988**, *29*, 297. (b) Brodbelt, J.; Maleknia, S.; Liou, C.-C.; Lagow, R. *J. Am. Chem. Soc.* **1991**, *113*, 5913. (c) Brodbelt, J.; Maleknia, S.; Lagow, R.; Lin, T. Y. *J. Chem. Soc., Chem. Commun.* **1991**, 1705. (d) Scheerder, J.; Fochi, M.; Engbersen, J. F. J.; Reinhoudt, D. N. *J. Org. Chem.* **1994**, *59*, 7815. (e) Savage, P. B.; Holmgren, S. K.; Gellman, S. H. *J. Am. Chem. Soc.* **1994**, *116*, 4069. (f) Worm, K.; Schmidtchen, F. P. *Angew. Chem., Int. Ed. Engl.* **1995**, *34*, 65. (g) Scheerder, J.; Engbersen, J. F. J.; Casnati, A.; Ungaro, R.; Reinhoudt, D. N. *J. Org. Chem.* **1995**, *60*, 6448. (h) Scheerder, J.; Engbersen, J. F. J.; Reinhoudt, D. N. *Recl. Trav. Chim. Pays-Bas* **1996**, *115*, 307. (i) Tamao, K.; Hayashi, T.; Ito, Y. *J. Organometallic Chem.* **1996**, *506*, 85. (j) Antonisse, M. M. G.; Snellink-Ruël, B. H. M.; Yigit, I.; Engbersen, J. F. J.; Reinhoudt, D. N. *J. Org. Chem.* **1997**, *62*, 9034. (k) Schmidtchen, F. P.; Berger, M. *Chem. Rev.* **1997**, *97*, 1609.

(24) (a) Bogdanov, B.; Peschke, M.; Tonner, D. S.; Szulejko, J. E.; McMahon, T. B. *Int. J. Mass Spectrom.* **1999**, *185/186/187*, 707 and references therein. (b) DeTuri, V. F.; Su, M. A.; Ervin, K. M. *J. Phys. Chem. A* **1999**, *103*, 1468. (c) DeTuri, V. F.; Ervin, K. M. *J. Phys. Chem. A* **1999**, *103*, 6911.

(25) Møller, C.; Plesset, M. S. *Phys. Rev.* **1934**, *46*, 618.

(26) (a) Lee, C.; Yang, W.; Parr, R. G. *Phys. Rev. B* **1988**, *37*, 785. (b) Becke, A. D. *J. Chem. Phys.* **1993**, *98*, 1372, 5648.

(27) (a) Bradforth, S. E.; Arnold, D. W.; Metz, R. B.; Weaver, A.; Neumark, D. M. *J. Phys. Chem.* **1991**, *95*, 8066. (b) Wladkowski, B. D.; East, A. L. L.; Mihalick, J. E.; Allen, W. D.; Brauman, J. I. *J. Chem. Phys.* **1994**, *100*, 2058. (c) Tanabe, F. K. J.; Morgon, N. H.; Riveros, J. M. *J. Phys. Chem.* **1996**, *100*, 2862. (d) Berthier, G.; Savinelli, R.; Pullman, A. *Int. J. Quantum. Chem.* **1997**, *63*, 567.

(28) Schlegel, H. B.; Frisch, M. J. *Theoretical and Computational Models for Organic Chemistry*; Formosinho, S. J., Ed., NATO-ASI Series C 339: Kluwer Academic Publications: The Netherlands, 1991; pp 5−33.

(29) Frisch, M. J.; Trucks, G. W.; Schlegel, H. B.; Gill, P. M. W.; Johnson, B. G.; Robb, M. A.;Cheeseman, J. R.; Keith, T.; Petersson, G. A.; Montgomery, J. A.; Raghavachari, K.;Al-Laham, M. A.; Zakrzewski, V. G.; Ortiz, J. V.; Foresman, J. B.; Peng, C. Y.; Ayala, P. Y.; Chen, W.; Wong, M. W.; Andres, J. L.; Replogle, E. S.; Gomperts, R.; Martin, R. L.; Fox, D. J.; Binkley, J. S.; Defrees, D. J.; Baker, J.; Stewart, J. P.; Head-Gordon, M.; Gonzales, C.; Pople, J. A. *Gaussian 94*, Revision B3; Gaussian Inc.: Pittsburgh PA, 1995.

(30) Frisch, M. J.; Trucks, G. W.; Schlegel, H. B.; Scuseria, G. E.; Robb, M. A.; Cheeseman, J. R.; Zakrzewski, V. G.; Montgomery, J. A., Jr.; Stratmann, R. E.; Burant, J. C.; Dapprich, S.; Millam, J. M.; Daniels, A. D.; Kudin, K. N.; Strain, M. C.; Farkas, O.; Tomasi, J.; Barone, V.; Cossi, M.; Cammi, R.; Mennucci, B.; Pomelli, C.; Adamo, C.;Clifford, S.; Ochterski, J.; Petersson, G. A.; Ayala, P. Y.; Cui, Q.; Morokuma, K.;Malick, D. K.; Rabuck, A. D.; Raghavachari, K.; Foresman, J. B.; Cioslowski, J.; Ortiz, J. V.; Baboul, A. G.; Stefanov, B. B.; Liu, G.; Liashenko, A.; Piskorz, P.; Komaromi, I.; Gomperts, R.; Martin, R. L.; Fox, D. J.; Keith, T.; Al-Laham, M. A.;Peng, C. Y.; Nanayakkara, A.; Gonzalez, C.; Challacombe, M.; Gill, M. W.; Johnson, B.; Chen, W.; Wong, M. W.; Andres, J. L.; Gonzalez, C.; Head-Gordon, M.; Replogle, E. S.; Pople, J. A. *Gaussian 98*, Revision A.7; Gaussian, Inc.: Pittsburgh PA, 1998.

(31) (a) Krishnan, R.; Binkley, J. S.; Seeger, R.; Pople, J. A. *J. Chem. Phys.* **1980**, *72*, 650. (b) Clark, T.; Chandrasekhar, J.; Schleyer, P. von. R. *J. Comput. Chem.* **1983**, *4*, 294.

(32) (a) Head-Gordon, M.; Pople, J. A.; Frisch, M. J. *Chem. Phys. Lett.* **1988**, *153*, 503. (b) Frisch, M. J.; Head-Gordon, M.; Pople, J. A. *Chem. Phys. Lett.* **1990**, *166*, 275. (c) Frisch, M. J.; Head-Gordon, M.; Pople, J. A. *Chem. Phys. Lett.* **1990**, *166*, 280.

(33) (a) Gill, P. M. W.; Johnson, B. G.; Pople, J. A.; Frisch, M. J. *Chem. Phys. Lett.* **1992**, *197*, 499. (b) Frisch, M. J.; Pople, J. A.; Binkley, J. S. *J. Chem. Phys.* **1984**, *80*, 3265.

(34) (a) Scott, A. P.; Radom, L. *J. Phys. Chem.* **1996**, *100*, 16502. A value of 0.9489 was obtained by subtracting the scaling factor difference of MP2(fc)/6-31G(d) and MP2(full)/6-31G(d) (0.9434 and 0.9427, respectively) from the scaling factor of MP2(fc)/6-311G(d,p) (0.9496). (b) From a least-squares fit of unscaled MP2(full)/6-311++G(d,p) normal mode vibrational frequencies of CH_3OH against experimental frequencies, a scaling factor of 0.9454 was obtained ($\Delta\nu = 26 \pm 15$ cm^{-1} (0.9454) vs ($\Delta\nu = 27 \pm 16$ cm^{-1} (0.9489)).

(35) From a least-squares fit of unscaled B3LYP/6-311+G(d,p) normal mode vibrational frequencies of CH_3OH against experimental frequencies, a scaling factor of 0.9640 was obtained ($\Delta\nu = 28 \pm 12$ cm^{-1} (0.9640) vs $\Delta\nu = 50 \pm 59$ cm^{-1} (1.0000)).

(36) Hay, P. J.; Wadt, W. R. *J. Chem. Phys.* **1985**, *82*, 284.

(37) Bergner, A.; Dolg, M.; Kuechle, W.; Stoll, H.; Preuss, H. *Mol. Phys.* **1983**, *80*, 1431.

(38) LaJohn, L. A.; Christiansen, P. A.; Ross, R. B.; Atashroo, T.; Ermler, W. C. *J. Chem. Phys.* **1987**, *87*, 2812.

(39) Basis sets were obtained from the Extensible Computational Chemistry Environment Basis Set Database, Version 1.0, as developed and distributed by the Molecular Science Computing Facility, Environmental and Molecular Sciences Laboratory, which is part of the Pacific Northwest Laboratory, P.O. Box 999, Richland, WA 99352, and funded by the U.S. Department of Energy. The Pacific Northwest Laboratory is a multi-program laboratory operated by Battelle Memorial Institute for the U.S. Department of Energy under contract DE-AC06-76RLO 1830.

(40) (a) Reed, A. E.; Weinstock, R. B.; Weinhold, F. *J. Chem. Phys.* **1985**, *83*, 735. (b) Reed, A. E.; Curtiss, L. A.; Weinhold, F. *Chem. Rev.* **1988**, *88*, 899.

(41) Foresman, J. B.; Frisch, Æ. *Exploring Chemistry with Electronic Structure Methods*, 2nd ed.; Gaussian Inc.: Pittsburgh, PA, 1996; pp 134, 172.

(42) (a) Szulejko, J. E.; Wilkinson, F. E.; McMahon, T. B. *Proceedings of the 37th ASMS Conference on Mass Spectrometry and Allied Topics*, May 21−26, 1989, Miami Beach, Fl; 1988; p 333. (b) Hiraoka, K.; Yamabe, S. *Int. J. Mass Spectrom. Ion Processes* **1991**, *109*, 133. (**c**) Yang, Y.;

Linnert, H. V.; Riveros, J. M.; Williams, K. R.; Eyler, J. R. *J. Phys. Chem. A* **1997**, *101*, 2371. (d) Yamdagni, R.; Kebarle, P. *J. Am. Chem. Soc.* **1971**, *93*, 7139. (e) Yamdagni, R.; Payzant, J. D.; Kebarle, P. *Can. J. Chem.* **1973**, *51*, 2507. (f) Larson, J. W.; McMahon, T. B. *J. Am. Chem. Soc.* **1984**, *106*, 517. (g) Keesee, R. G.; Castleman, A. W., Jr. *Chem. Phys. Lett.* **1980**, *74*, 139. (h) Hiraoka, K.; Mizuse, S. *Chem. Phys.* **1987**, *118*, 457. (i) Evans, D. H.; Keesee, R. G.; Castleman, A. W., Jr. *J. Phys. Chem.* **1991**, *95*, 3558. (j) Kebarle, P. *Annu. Rev. Phys. Chem.* **1977**, 28. (k) Caldwell, G.; Kebarle, P. *J. Am. Chem. Soc.* **1984**, *106*, 967.

(43) Glukhovtsev, M. N.; Pross, A.; Radom, L. *J. Am. Chem. Soc.* **1995**, *117*, 2024.

(44) (a) v. Szentpaly, L.; Fuentealba, P.; Preuss H.; Stoll, H. *Chem. Phys. Lett.* **1982**, *93*, 555. (b) Leininger, T.; Nicklass, A.; Stoll, H.; Dolg M.; Schwerdtfeger, P. *J. Chem. Phys.* **1996**, *105*, 1052.

(45) Hu, W. P.; Truhlar, D. G. *J. Phys. Chem.* **1994**, *98*, 1049.

(46) (a) Glukhovtsev, M. N.; Pross, A.; McGrath, M. P.; Radom, L. *J. Chem. Phys.* **1995**, *103*, 1878. (b) Glukhovtsev, M. N.; Pross, A.; Radom, L. *J. Am. Chem. Soc.* **1995**, *117*, 2024. (c) Glukhovtsev, M. N.; Pross, A.; Radom, L. *J. Am. Chem. Soc.* **1996**, *118*, 6273.

(47) DeTuri, V. F. Personal communication.

(48) (a) Su, T.; Bower, M. T. *Int. J. Mass Spectrom. Ion Phys.* **1973**, *12*, 347. (b) Grabowski, J. J.; Bierbaum, V. M.; DePuy, C. H. *J. Am. Chem. Soc.* **1983**, *105*, 2565.

(49) Martin, J. D. D. Ph.D. Dissertation, University of Waterloo, 1998.

(50) Work in progress.

(51) Shimanouchi, T. *Tables of Molecular Vibrational Frequencies Consolidated Volume I*; National Bureau of Standards: Washington, DC, 1972; p 1.